

Versatile Fabrication of Intact Three-Dimensional Metallic Butterfly Wing Scales with Hierarchical Sub-micrometer Structures**

Yongwen Tan, Jiajun Gu,* Xining Zang, Wei Xu, Kaicheng Shi, Linhua Xu, and Di Zhang*

Three-dimensional (3D) metallic microstructures with well-controlled hierarchical morphologies down to the sub-micrometer scale have attracted considerable attention.^[1] These structures have broad applications owing to their unique optical,^[2a] electronic,^[2b] magnetic,^[2c] thermal,^[2d,e] and catalytic^[2f] properties, which can be modulated by their intrinsic microstructures. Such structures, however, are quite difficult to prepare by traditional methods. One promising route to create these metallic structures is direct replication from hierarchical structures of various natural species. Metals have been physically deposited onto biological structures to fabricate metallic structures through physical vapor deposition (PVD).^[3] However, the line-of-sight nature of PVD prevented a complete replication of the biotemplates' original 3D morphologies.^[4] Some groups elegantly converted natural inorganic structures such as diatom frustules into metals (Ag, Au, Pd) using wet-chemical processes,^[4] but many natural species with functional structures are composed of organic materials. Versatile synthesis of metallic structures using organic-based natural species' intact, 3D, and hierarchical sub-micrometer morphologies as templates is thus needed.

Herein we present a versatile route (selective surface functionalization and subsequent electroless deposition) to generate metallic replicas of the intact 3D organic butterfly (*Euploea mulciber*) wing scales. This method can replicate the original chitin-based scales' morphology in at least seven important metals, including cobalt, nickel, copper, palladium, silver, platinum, and gold (Figure 1 and Figure 2). Significantly, using the synthetic Au scale as a surface-enhanced Raman scattering (SERS) substrate, the detectable analyte

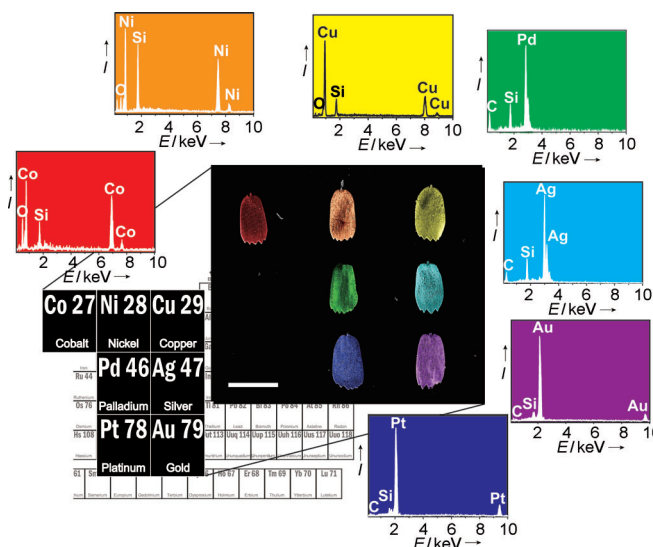


Figure 1. SEM element mapping images of seven metallic wing-scale replicas. All of the metallic replicas were imaged under high vacuum without metal sputtering that was needed for original nonconductive butterfly scale samples. Silicon signals originate from the Si wafer substrate, and slight oxidation occurs for the Co and Ni replicas (in the Supporting Information it is also mentioned that Cu is slightly oxidized). Au NPs as catalysts could not be identified in the replicas (except for the Au scale) owing to their small numbers in comparison with grains in the continuous deposited metal layers. Pseudo colors based on mapping data were generated directly using the software Microanalysis Suite (18d + SPS, Oxford Instruments Inca). Scale bar: 50 μm .

concentration (Rhodamine 6G, 10^{-13}M) can be one order of magnitude lower than using commercial substrates (Klarite). To our knowledge, this work is the first demonstration of the conversion of intact hierarchical 3D butterfly structures on a sub-micrometer level into metallic replicas. It should be noted that butterflies belong to the order *Lepidoptera* (Latin word for “scaly wing”, including butterflies and moths) that comprises an estimated 174250 species.^[5] A given species usually has more than one type of wing scale,^[6] and such huge morphological diversity offers a vast structure pool for biotemplate selection (e.g., photonic crystal design).^[7a] In addition, chitin, the main component of butterfly wing scales, is one of the richest natural macromolecular compounds.^[8] Therefore, this approach can be extended to replicate other chitin-based biostructures, including fungi cell walls, exoskeletons of insects^[9a,b] and arthropods (e.g., crabs and lobsters),^[9c] radulas of mollusks (e.g., snails), and beaks of cephalopods (e.g., squids^[9d] and octopuses).

The fabrication route described herein consists of three steps (see Scheme S1 in the Supporting Information): 1) func-

[*] Dr. Y. W. Tan, Prof. Dr. J.-J. Gu,^[†] X. N. Zang,^[†] W. Xu,^[†] K. C. Shi,^[†] L. H. Xu,^[†] Prof. Dr. D. Zhang
State Key Laboratory of Metal Matrix Composites
Shanghai Jiao Tong University
800 Dongchuan Road, Shanghai 200240 (P.R. China)
E-mail: gujiajun@sjtu.edu.cn
zhangdi@sjtu.edu.cn

[†] These authors contributed equally to this work.

[**] We thank Prof. S. M. Zhu, Shanghai Jiao Tong University, for discussion. This work was supported by the 973 National Project (No. 2011CB922200), Shanghai Science and Technology Committee (10JC1407600), Sino-French Project of MOST of China (No. 2009DFA52410), Sino-Finland International Program of Shanghai (No. 09520703400), and Sino-Australia Project of MOST of China (2010DFA52550). X.Z., W.X., K.S., and L.X. appreciate the financial support from the Third Shanghai Innovation Experiment Program for Undergraduate Students, and the Participation in Research Program (PRP) of Shanghai Jiao Tong University.

Supporting information for this article is available on the WWW under <http://dx.doi.org/10.1002/anie.201103505>.

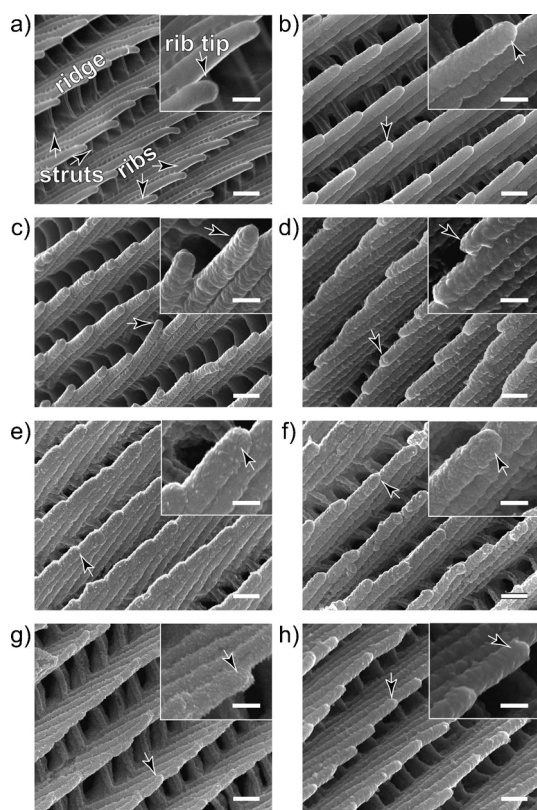


Figure 2. SEM images of a) an original wing scale, b) Co, c) Ni, d) Cu, e) Pd, f) Ag, g) Pt, and h) Au replicas. Scale main ridges, struts, and ribs are marked in (a). Insets show morphologies with higher magnification. Arrows in (b–h) denote the rib tips of the metallic replicas. Scale bars: 500, 250 nm (insets).

tionalization of a chitin-based surface with Au nanoparticles (NPs), 2) standard electroless deposition of one of seven metals onto the scales at modest temperatures, and 3) selective removal of the original chitin-based biotemplates. Steps (1) and (3) are identical for all seven metallic replicas, thus suggesting the versatility of this route. Figure 1 shows a scanning electron element mapping image of seven synthesized metallic scales manually manipulated and arranged together on a silicon wafer. Detailed energy-dispersive X-ray spectrometry (EDS) results for each replica verify the successful conversion of the chemical composition, which is confirmed by X-ray diffraction (XRD) analysis as well (see Figure S1 in the Supporting Information). As revealed by the XRD results, the average grain size is different for various metal samples. It ranges from approximately 4 nm (Ni) to 20 nm (Ag) depending on the metal, promising the replication of wing scales' subtle morphologies down to the sub-micrometer scale. Slight oxidation could be identified in the samples of Co, Ni, and Cu (XRD results, Figure S1 in the Supporting Information) because of their small grain size and exposure to air.

To evaluate the conformity between original butterfly scales and the final metallic replicas, the morphologies of metallic scales are compared with their original counterpart in Figure 2 (higher magnification) and Figure S2 in the Supporting Information (lower magnification). Like many other

butterflies and moths,^[6] the original scale of *E. multicolor* with hierarchical morphology usually contains three levels of periodicity. The largest size of approximately 700 nm is defined by the space between two adjacent main ridges (Figure 2a), while a smaller one (ca. 380 nm) describes the distance between struts^[7b,d] (top view). Much finer structures (ribs^[7b,d]) can be identified on the individual ridges, with a period of approximately 100 nm. Because of the individual differences of single scales, these values could vary slightly. Through this wet-chemical synthesis route, all these periodicities were topologically replicated (Figure 2b–h) for all the metallic replicas owing to their small grain size, and the capability of metal ions to get into the blind corners of intricate biological structures. The gap distances decrease somewhat because of the metal coating thickness. The layer thickness is approximately 20–50 nm for main ridges and struts, resulting in shrinkage of approximately 6–14 % and 11–26 % for the spaces between main ridges and between struts, respectively. These dimensions can be further tuned by modifying the deposition conditions, which will affect the metallic replicas' properties (e.g., surface enhancement of Raman signals, which will be reported elsewhere). Using an SEM stage tilt (45° against the length direction of main ridges), the layer thickness for ribs is roughly estimated to be 20–30 nm, which causes 40–60 % shrinkage in the space between ribs, as viewed parallel to the bisecting plane between main ridge walls and the substrate surface. More precise dimensional measurement of the replicas' rib period, which is based on cross-section samples prepared using focused ion beam milling, is currently underway. Lower-magnification images ($\times 10000$, Figure S2 in the Supporting Information) reveal homogeneous metal deposition over a large-scale surface area.

The metallic replicas were further manually broken under an optical stereomicroscope with a needle for the observation of their internal structures (Figure 3). The 3D structures from original scales^[6a] are well-maintained. As described by many previous studies,^[6,7] the scale struts actually consist of vertical and horizontal struts, which support and connect the main ridges. A close-up view of the structures (right column, Figure 3) shows that some parts of the replicas are hollow, owing to the removal of the original chitin-based organisms.

In generating replicas from biotemplates, calcination has been used frequently to fabricate oxide replicas.^[7] Unlike grains of oxides and inorganic ternary compounds, metal particles have higher surface energies and tend to coarsen easily at high temperatures. Such coarsening makes the calcination process unsuitable to convert biotemplates with sub-micrometer morphologies into metals.^[7] In comparison, electroless deposition is a reliable method for insulating-surface metallization. Although a direct electroless deposition of metal coatings onto organic surfaces is quite difficult, it has been successfully used to apply Ag,^[10a,b] Au,^[10c] Cu,^[10d] and Ni^[11a–c] coatings to pattern polymers through surface-functionalization processes. Metals such as Au^[10b] and Pd^[11] and compounds such as SnCl₂^[10a,d] have been successfully utilized to activate the polymer surface before deposition. However, natural butterfly wing scales are actually composites composed of chitin and a small amount of protein with lots of OH,

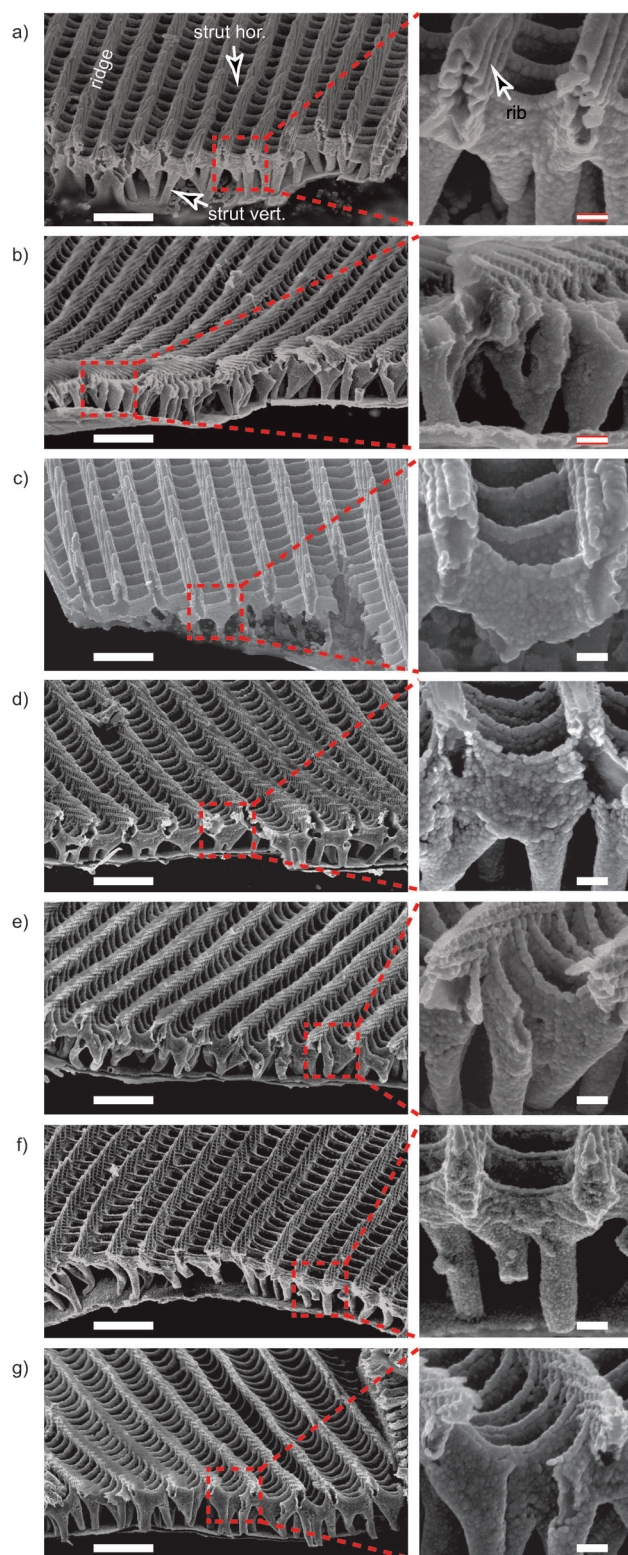


Figure 3. Cross-section SEM images of a) Co, b) Ni, c) Cu, d) Pd, e) Ag, f) Pt, and g) Au replicas, respectively. Scale main ridges, struts (vertical and horizontal), and ribs are marked in (a). Scale bars: 2 μm (left column), 250 nm (right column).

NHCOCH_3 , and NH_2 groups.^[12] To achieve uniform and complete metal coatings at a sub-micrometer level on the surface of these composites with hierarchical 3D morpholo-

gies, we used ethanediamine (EDA), containing two amino groups, to aminate the scale surface first (Scheme S1 in the Supporting Information). One amino group of EDA would bind with an OH group on the chitin-based surface by nucleophilic attack, leaving the other in complex with Au^{III} .^[10b] Au nanoparticles (NPs) were subsequently formed at the aminated scale surface by sodium borohydride (NaBH_4) reduction of the coordinated Au^{III} , which acted as catalyst for the subsequent electroless metal deposition. A detailed analysis of the functionalization process based on infrared absorption spectra is provided in the Supporting Information (Figure S3).

Continuous replication was achieved through further deposition of Ag, Au, Co, Cu, Ni, Pd, and Pt in corresponding solutions onto the functionalized scale surfaces by standard electroless deposition processes. Detailed plating solutions and reaction conditions are listed in Table S1 in the Supporting Information.^[10,11a,13] All of these deposition processes were carried out at room temperature (except Pt, at 50 °C), to suppress the coarsening of the metallic microstructures induced by their high surface energies. After the electroless deposition on the bioorganic surfaces, the chitin-based wing scales were finally removed using H_3PO_4 (see Figure S4 in the Supporting Information).^[14] The metallic butterfly wing scales were thus fabricated.

Although many applications (e.g. in catalysis and magnetism) of these unique metallic scales are still under study at present, we demonstrate herein how these mass-producible metallic structures can substantially enhance Raman signals of the analyte on them with a detection sensitivity one order of magnitude higher and at a cost one order of magnitude lower than their commercial counterpart (see Figure 4 and Figure S5 in the Supporting Information). Surface-enhanced Raman scattering (SERS) has been attracting increasing interest since the 1970s owing to its ability to increase the intensity of Raman signals that are usually weakly scattered and thus has broad applications in chemistry, the life sciences, and physics.^[15,16] This phenomenon originates from the roughened surface of a metal substrate, which generates highly localized surface plasmon resonance and in turn yields a significant Raman signal enhancement.^[16] Although the mechanism of SERS has not yet been totally understood, SERS substrates as consumables with super sensitivity, excellent reproducibility, and low cost are highly anticipated. Much evidence has indicated that 3D noble-metal superstructures help enhance the SERS by electromagnetic amplification controlled by sub-micrometer structures.^[16g] Garrett et al. physically deposited Au onto butterfly wing surfaces (referred to hereafter as physical scales) to fabricate SERS substrates.^[3d] However, the drawbacks of PVD as mentioned above would inhibit a full utilization of original biotemplates' 3D morphologies. In comparison, using the unique metallic structures (or "chemical scales") synthesized with the chemical approach reported herein as SERS substrates, the detectable lower limit of analyte concentration can surprisingly decrease by even one order of magnitude (Rhodamine 6G, 10^{-13} M), as compared with commercial substrates (10^{-12} M , Klarite, Renishaw Diagnostics), and with studies published very recently.^[16a-c] Moreover, the lowest detectable

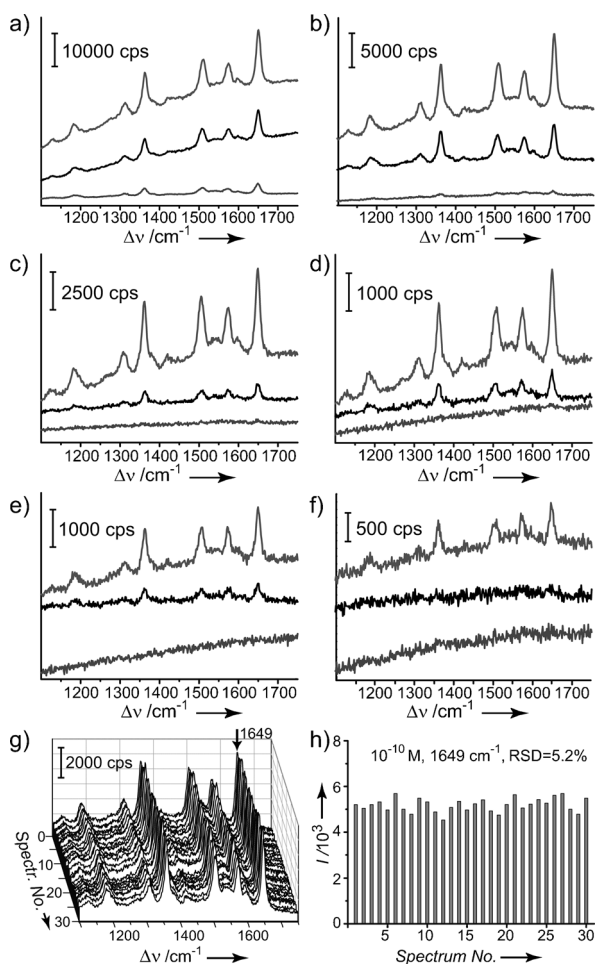


Figure 4. a–f) Comparison of Raman signals from R6G on three Au SERS diagnostic substrates. R6G concentrations: a) 10^{-6} M; b) 10^{-8} M; c) 10^{-10} M; d) 10^{-11} M; e) 10^{-12} M; f) 10^{-13} M. Data from top to bottom in each diagram were collected on Au butterfly scales chemically synthesized in this work (chemical scales), commercial SERS substrate (Klarite), and Au scales prepared by simple physical deposition (physical scales). The original scales were chosen from the blue ones on *E. multicolor*'s dorsal wing surface. Note that the diagnostic sensitivity of chemical scales is one order and four orders of magnitude higher than the commercial Klarite substrates and physical scales, respectively. g) Raman signals (R6G, 10^{-10} M) obtained at thirty different spots from ten Au chemical scales. Note that the concentration chosen here for reproducibility evaluation is one order of magnitude lower than the one reported in very recent work (10^{-9} M).^[16a] h) Intensity variation of the peak at 1649 cm^{-1} in (g).

R6G concentration on chemical scales drastically decreases by four orders of magnitude as compared with the use of Au scales that were prepared by simple physical deposition (physical scales).^[3d] Although there is currently no direct experimental evidence demonstrating that the chemical scales can be directly used in single-molecule detection, we have roughly estimated the number of molecules within the detected area using a method presented in reference [16a]. We applied R6G solution (1 mL, 10^{-13} M in ethanol, ca. 6×10^7 R6G molecules) onto the chemical scale surface for detection. The liquid drops finally spread out with a diameter of approximately 1 cm, while the cross section of the laser

beam used for Raman detection was approximately $2\text{ }\mu\text{m}$ in diameter. Supposing that these 6×10^7 R6G molecules were adsorbed evenly onto the 1 cm^2 area,^[16a] the molecular signals collected for Raman measurement were thus from less than ten molecules. Moreover, in Figure 4g,h, we measured Raman signals at thirty randomly chosen spots from ten chemical scales to evaluate the reproducibility. The relative standard deviation (RSD) is 5.2%, which is comparable to^[16a,d] or even better than^[16c,e,f] those reported in very recent studies. Detailed analyses on how various scale morphologies (from different butterfly species) can affect the localized surface plasmon resonance are currently underway and may help further enhance the Raman signals of analytes by aiding selection of proper types of scales as biotemplates for replication.

To demonstrate how the structures synthesized herein can be mass-manufactured for Raman measurement, we present the Raman spectra acquired on a whole Au wing of *E. Multiciber* as SERS substrate (Figure S5 in the Supporting Information). Again, the R6G solution of 10^{-13} M is detectable. Since the cost of the Au wing that is tailored into $4 \times 4\text{ mm}^2$ is about one order of magnitude cheaper (ca. \$2.50, providing more than 10000 single scales) than a consumable commercial substrate (Klarite, $4 \times 4\text{ mm}^2$), and the Au wings (scales) can be prepared within thirteen hours without the removal of original chitin in an ordinary laboratory for Raman detection, the approach reported herein can make ultrasensitive Raman analysis (near-single-molecule detection) with excellent reproducibility a routine diagnostic method for chemists, life scientists, and physicists.

In conclusion, we have developed a versatile approach to prepare intact 3D metallic replicas (Ag, Au, Co, Cu, Ni, Pd, and Pt) down to sub-micrometer level of butterfly wing scales. Through selective surface functionalization and standard electroless deposition, a homogeneous and morphology-preserving replication of original scales' intricate 3D microstructures is achieved. It should be noted that the scales' full 3D hierarchical structures are intact, especially after the removal of the biotemplates. Significantly, using the novel Au butterfly wings (or scales) with these superstructures as SERS substrates, a detectable lower limit of R6G concentration that is one order of magnitude lower than with the commercial counterpart has been achieved. This work provides a general strategy for replicating chitin-based structures with fine and hierarchical 3D morphologies using a wide variety of metals with magnetic, optical, catalytic, electronic, and thermal applications. A portal to intact 3D metallic *Lepidopterans* (butterflies and moths), which contains approximately 174250 species and even more types of wing scales, is now open.

Experimental Section

The detailed synthesis route is provided in the Supporting Information. Scanning electron microscopy was carried out using a field-emission SEM instrument (Quanta 250 from FEI, 20 kV) equipped with EDS analysis capability (Oxford Instruments, 80 mm² detector). X-ray diffraction measurements were conducted using a D/max-2550 instrument ($\text{Cu}_{\text{K}\alpha}$) from Rigaku Corporation. Scales (ca. 0.5 g) were scratched off from the metal-coated wings and were treated with H_3PO_4 for the XRD measurement. Infrared absorption spectra were

recorded using a Perkin–Elmer Spectrum 100 instrument with samples ground to powders and compressed into KBr pellets.

To evaluate the SERS efficiency of Au chemical scales, R6G solution (1 mL) in ethyl alcohol (10^{-6} – 10^{-13} M, respectively) was drop-evaporated in ten 0.1 mL portions onto the substrates, which were then dried under ambient conditions before tests. Raman measurements were then conducted under a Renishaw inVia Raman microscope operated with an Ar ion laser (514.5 nm). The laser had a power of 2 mW at the sample surface, with 2 μ m in beam diameter. The integration time was 10 s. The reproducibility evaluation was carried out at thirty randomly chosen spots from ten Au chemical scales. Commercial Klarite substrates were purchased from Renishaw Diagnostics. To prepare physical scales, Au was physically deposited onto the wing scale surface (4 min with a deposition rate of 20 nm min $^{-1}$, the optimized synthesis condition as reported in Ref. [3d]) using a Hitachi Ion Sputter Coater (E-1045). Raman signals of R6G on Klarite substrates and on physical scales were acquired under the same experimental conditions as on chemical scales for comparison.

Received: May 22, 2011

Published online: July 21, 2011

Keywords: biological templates · metals · nanostructures · surface-enhanced Raman spectroscopy · template synthesis

- [1] a) L. Lu, I. Randjelovic, R. Capek, N. Gaponik, J. Yang, H. Zhang, A. Eychmüller, *Chem. Mater.* **2005**, *17*, 5731–5736; b) Y.-S. Chen, A. Tal, D. B. Torrance, S. M. Kuebler, *Adv. Funct. Mater.* **2006**, *16*, 1739–1744; c) J. Zhang, Y. Li, X. Zhang, B. Yang, *Adv. Mater.* **2010**, *22*, 4249–4269.
- [2] a) X. Liu, C. Sun, P. Jiang, *Chem. Mater.* **2010**, *22*, 1768–1775; b) Y. Deng, W. Huang, X. Chen, Z. Li, *Electrochem. Commun.* **2008**, *10*, 810–813; c) G. Ctistis, E. Papaioannou, P. Patoka, J. Gutek, P. Fumagalli, M. Giersig, *Nano Lett.* **2009**, *9*, 1–6; d) J. H. Lee, J. C. W. Lee, W. Leung, M. Li, K. Constant, C. T. Chan, K.-M. Ho, *Adv. Mater.* **2008**, *20*, 3244–3247; e) P. Nagpal, S. E. Han, A. Stein, D. J. Norris, *Nano Lett.* **2008**, *8*, 3238–3243; f) R. Wang, C. Wang, W. B. Cai, Y. Ding, *Adv. Mater.* **2010**, *22*, 1845–1848.
- [3] a) D. Losic, J. G. Mitchell, N. H. Voelcker, *Chem. Commun.* **2005**, 4905–4907; b) D. Losic, J. G. Mitchell, N. H. Voelcker, *New J. Chem.* **2006**, *30*, 908–914; c) E. K. Payne, N. L. Rosi, C. Xue, C. A. Mirkin, *Angew. Chem.* **2005**, *117*, 5192–5195; *Angew. Chem. Int. Ed.* **2005**, *44*, 5064–5067; d) N. L. Garrett, P. Vukusic, F. Ogrin, E. Sirotkin, C. P. Winlove, J. Moger, *J. Biophotonics* **2009**, *2*, 157–166.
- [4] a) Z. Bao, E. M. Ernst, S. Yoo, K. H. Sandhage, *Adv. Mater.* **2009**, *21*, 474–478; b) Y. Yu, J. Addai-Mensah, D. Losic, *Langmuir* **2010**, *26*, 14068–14072.
- [5] J. Mallet, “Taxonomy of Lepidoptera: the scale of the problem”. The Lepidoptera Taxome Project, University College London, UK, to be found under <http://www.ucl.ac.uk/taxome/lepnos.html>. **2011**.
- [6] a) A. L. Ingram, A. R. Parker, *Philos. Trans. R. Soc. London Ser. B* **2008**, *363*, 2465–2480; b) V. Saranathan, C. O. Osujib, S. G. J. Mochrie, H. Noh, S. Narayanan, A. Sandy, E. R. Dufresne, R. O. Prum, *Proc. Natl. Acad. Sci. USA* **2010**, *107*, 11676–11681; c) P. Vukusic, J. R. Sambles, *Nature* **2003**, *424*, 852–855.
- [7] a) J. Huang, X. Wang, Z. L. Wang, *Nano Lett.* **2006**, *6*, 2325–2331; b) M. R. Weatherspoon, Y. Cai, M. Crne, M. Srinivasarao, K. H. Sandhage, *Angew. Chem.* **2008**, *120*, 8039–8041; *Angew. Chem. Int. Ed.* **2008**, *47*, 7921–7923; c) W. Zhang, D. Zhang, T. X. Fan, J.-J. Gu, J. Ding, H. Wang, Q. X. Guo, H. Ogawa, *Chem. Mater.* **2009**, *21*, 33–40; d) J. P. Vernon, Y. Fang, Y. Cai, K. H. Sandhage, *Angew. Chem.* **2010**, *122*, 7931–7934; *Angew. Chem. Int. Ed.* **2010**, *49*, 7765–7768; e) W. Zhang, D. Zhang, T. X. Fan, J. Ding, Q. X. Guo, H. Ogawa, *Microporous Mesoporous Mater.* **2006**, *92*, 227–233; f) X. Y. Liu, S. M. Zhu, D. Zhang, Z. X. Chen, *Mater. Lett.* **2010**, *64*, 2745–2747.
- [8] A. P. Mathew, M. P. G. Laborie, K. Oksman, *Biomacromolecules* **2009**, *10*, 1627–1632.
- [9] a) A. R. Parker, V. L. Welch, D. Driver, N. Martini, *Nature* **2003**, *426*, 786–787; b) V. Sharma, M. Crne, J. O. Park, M. Srinivasarao, *Science* **2009**, *325*, 449–451; c) D. Aurognzeb, *J. Appl. Phys.* **2009**, *105*, 056108; d) J. J. Walish, Y. Kang, R. A. Mickiewicz, E. L. Thomas, *Adv. Mater.* **2009**, *21*, 3078–3081.
- [10] a) Z. Chen, P. Zhan, Z. Wang, J. Zhang, W. Zhang, N. Ming, C. T. Chan, P. Sheng, *Adv. Mater.* **2004**, *16*, 417–422; b) Y.-S. Chen, A. Tal, S. M. Kuebler, *Chem. Mater.* **2007**, *19*, 3858–3860; c) Z. Liang, A. Susha, F. Caruso, *Chem. Mater.* **2003**, *15*, 3176–3183; d) S. K. Smoukov, K. J. M. Bishop, C. J. Campbell, B. A. Grzybowski, *Adv. Mater.* **2005**, *17*, 751–755.
- [11] a) J. R. Lancaster, J. Jehani, G. T. Carroll, Y. Chen, N. J. Turro, J. T. Koberstein, *Chem. Mater.* **2008**, *20*, 6583–6585; b) P. Jenvanitpanjakul, S. Shiangawa, *J. Porous Mater.* **1999**, *6*, 239–246; c) E. Renbutsu, S. Okabe, Y. Omura, F. Nakatsubo, S. Minami, H. Saimoto, Y. Shigemasa, *Carbohydr. Polym.* **2007**, *69*, 697–706; d) Y. Omura, E. Renbutsu, M. Morimoto, H. Saimoto, Y. Shigemasa, *Polym. Adv. Technol.* **2003**, *14*, 35–39; e) E. Renbutsu, S. Okabe, Y. Omura, F. Nakatsubo, S. Minami, Y. Shigemasa, H. Saimoto, *Int. J. Biol. Macromol.* **2008**, *43*, 62–68; f) D. Zabetakis, W. J. Dressick, *ACS Appl. Mater. Interfaces* **2009**, *1*, 4–25.
- [12] J. H. Chen, Y. C. Lee, M. T. Tang, Y. F. Song, *AIP Conf. Proc.* **2007**, *879*, 1940–1943.
- [13] a) W. Dong, H. Dong, Z. Wang, P. Zhan, Z. Yu, X. Zhao, Y. Zhu, N. Ming, *Adv. Mater.* **2006**, *18*, 755–759; b) A. Tal, Y.-S. Chen, H. E. W. Williams, R. C. Rumpf, S. M. Kuebler, *Opt. Express* **2007**, *15*, 18283–18293; c) M. Mertig, R. Kirsch, W. Pompe, *Appl. Phys. A* **1998**, *66*, S723–S727; d) Z. Shi, S. Wu, J. A. Szpunar, *Nanotechnology* **2006**, *17*, 2161–2166.
- [14] a) M. Vincendon, *Carbohydr. Polym.* **1997**, *32*, 233–237; b) A. Lakhtakia, R. J. Martín-Palma, M. A. Motyka, C. G. Pantano, *Bioinspiration Biomimetics* **2009**, *4*, 034001.
- [15] a) M. Fleischmann, P. J. Hendra, A. J. McQuillan, *Chem. Phys. Lett.* **1974**, *26*, 163–166; b) D. L. Jeanmaire, R. P. Van Duyne, *J. Electroanal. Chem.* **1977**, *84*, 1–20.
- [16] a) Y. Zhao, X. J. Zhang, J. Ye, L. M. Chen, S. P. Lau, W. J. Zhang, S. T. Lee, *ACS Nano* **2011**, *5*, 3027–3033; b) Z. Huang, G. Meng, Q. Huang, Y. Yang, C. Zhu, C. Tang, *Adv. Mater.* **2010**, *22*, 4136–4139; c) D. Choi, Y. Choi, S. Hong, T. Kang, L. P. Lee, *Small* **2010**, *6*, 1741–1744; d) A. Kamińska, I. Dziecielewska, J. L. Weyher, J. Waluk, S. Gawinkowski, V. Sashuk, M. Fiałkowski, M. Sawicka, T. Suski, S. Porowski, R. Hołyst, *J. Mater. Chem.* **2011**, *21*, 8662–8669; e) D. He, B. Hu, Q. F. Yao, K. Wang, S. H. Yu, *ACS Nano* **2009**, *3*, 3993–4002; f) X. F. Liu, N. C. Linn, C. H. Sun, P. Jiang, *Phys. Chem. Chem. Phys.* **2010**, *12*, 1379–1387; g) Z. N. Zhu, H. F. Meng, W. J. Liu, X. F. Liu, J. X. Gong, X. H. Qiu, L. Jiang, D. Wang, Z. Y. Tang, *Angew. Chem.* **2011**, *123*, 1631–1634; *Angew. Chem. Int. Ed.* **2011**, *50*, 1593–1596.